Journal of Fluorescence, Vol. 15, No. 5, September 2005 (© 2005)
DOI: 10.1007/s10895-005-2982-8

Fluorescence Dynamics of DNA Condensed by the Molecular Crowding Agent Poly(Ethylene Glycol)

Mamata H. Kombrabail[1] and G. Krishnamoorthy[1,2]

Received June 22, 2005; accepted July 26, 2005

Condensation of extended DNA into compact structures is encountered in a variety of situations, both natural and artificial. While condensation of DNA has been routinely carried out by the use of multivalent cations, cationic lipids, detergents, and polyvalent cationic polymers, the use of molecular crowding agents in condensing DNA is rather striking. In this work, we have studied the dynamics of plasmid DNA condensed in the presence of a molecular crowding agent, polyethylene glycol (PEG). Steady-state and time-resolved fluorescence of the recently established condensation-indicating DNA binder, YOYO-1 [G. Krishnamoorthy, G. Duportail, and Y. Mely (2002), Biochemistry **41**, 15277–15287] was used in inferring the dynamic aspects of DNA condensates. It is shown that DNA condensed by PEG is more flexible and less compact when compared to DNA condensed by binding agents such as polyethyleneimine. The relevance of such differences in dynamics toward functional aspects of condensed DNA is discussed.

KEY WORDS: Condensed DNA; fluorescence anisotropy decay; polyethyleneglycol; molecular crowding.

INTRODUCTION

Condensation of extended DNA polymers into compact structures is relevant in both natural cellular processes such as DNA packaging in chromosomes [1] and phage heads [2] and in artificial gene therapy systems [3–6]. DNA is a highly charged polyelectrolyte, and therefore its compaction is nontrivial [7,8]. *In-vitro* condensation of DNA is generally achieved by neutralizing the negative charges on the DNA by one of several agents such as polycations [9–11], cationic lipids [12,13] and detergents [11,14], peptides [15], and multivalent metal ions [11,16]. Experimental observations point out that condensation of DNA occurs when nearly 90% of negative charges of DNA backbone phosphates are neutralized [8]. Although this could be rationalized by Manning's counterion condensation theory [17], the origin of the overall driving force behind condensation of DNA is still disputed. The total free energy ΔG_{cond} associated with the condensation process is contributed by several components such as ΔG terms associated with DNA bending, mixing, and demixing with solvent, electrostatic interactions, fluctuation of molecular interactions, and hydration forces [18,19]. The relative contribution of these various terms resulting in favorable ΔG_{cond} is still unknown. The absence of quantitative predictions on DNA condensation is even more stark when observations such as DNA condensation induced by solid surfaces [20] are taken into account.

Condensation of DNA has also been achieved by osmotic exclusion or macromolecular crowding offered by a variety of noninteracting polymers such as polyethylene glycol (PEG) [21–24]. This neutral polymer forms directional bonds with water and adopts higher order intrachain structure [22]. PEG is used to precipitate DNA from cell extracts and to improve the action of ligases and topoisomerases on high molecular weight DNA [25]. Steric factors offered by solvent-exclusion could be the driving force behind condensation of DNA by polymers such as PEG. The collapse of DNA in PEG solution is connected with the effect of immiscibility of stiff chains

[1] Department of Chemical Sciences, Tata Institute of Fundamental Research, Mumbai, India.
[2] To whom correspondence should be addressed. E-mail: gk@tifr.res.in

1053-0509/05/0900-0741/0 © 2005 Springer Science+Business Media, Inc.

(DNA) and flexible coils (PEG) [7]. Influence of macromolecular crowding has been implicated in several other processes such as protein folding [26] and molecular interactions [27] in cellular environments. Cell interior is packed with a large variety of macromolecules. Though their individual concentration is low, but when put together they occupy substantial fraction of the volume of the cell. Such a milieu exerts osmotic exclusion force on other macromolecules favoring processes such as molecular association [28,29]. Thus, condensation of DNA induced by molecular crowding could be thought of as a process, which might occur, naturally in cellular milieu. Furthermore, condensation of DNA by molecular crowding agents could be used as an alternate approach in gene delivery systems limited by cytotoxicity caused by excess of condensing agents such as cationic polymers [30,31].

DNA condensation has been studied using various techniques such as circular dichroism [25], dynamic light scattering [29], fluorescence microscopy [7,23,24] and spectroscopy [11,15], stopped flow and field jump experiments using scattered light [32], and Atomic Force Microscopy [20,33]. Condensed DNA takes various forms such as rods, fibers, and flexible circles. However, toroids are the most commonly encountered shape [20,33]. In contrast to the wealth of information available on the DNA condensation process, the level of information on the dynamics of condensed DNA is very scarce.

How do the DNA molecules condensed by either charge neutralizing agents such as cationic polymers/detergents or molecular crowding agents such as PEG compare with each other? Are their structure and dynamics similar to each other? If not similar, what are the essential differences? These are the questions, which prompted us to undertake the present work. In this work, we use the bis-intercalating dye YOYO-1 [11,15] to study the structure and dynamics of DNA condensed by PEG. We compare the dynamics of base and the backbone of DNA condensed by either class of condensing agents. Our results show that DNA condensed by PEG is less compact and less rigid when compared to DNA condensed by binding agents.

MATERIALS AND METHODS

pBsks plasmid DNA (3 kbp) was extracted by alkaline lysis method. YOYO-1 (491/509) was obtained from Molecular Probes Inc., and PEG, CTAB, glycerol, and HEPES were from Sigma Chemicals. Branched chain PEI (25 kDa) was a gift from Prof. J-P Behr, Illkirch, France.

Plasmid DNA-YOYO-1 complexes were made by mixing equal volumes of solutions of DNA and YOYO-1 in 20 mM HEPES pH 7.4 and 500 mM NaCl. The mixed solution was incubated at room temperature for at least 3 hr before use. This procedure ensured uniform distribution of YOYO-1. D:P ratio varied from 1:50 to 1:10000 depending on the experiment. PEG was dissolved in 20 mM HEPES pH 7.4 and 500 mM NaCl. The final concentration of PEG in solution was from 2 mg/mL to 200 mg/mL. PEG solution was mixed with the preincubated DNA-YOYO-1 solution to make the required concentration. This mixture was further incubated for 1 hr at room temperature. Details of typical concentrations of PEG used are given in figure legends. Solutions DNA-YOYO-1 without PEG were used as control. The complexes of plasmid DNA-YOYO-1 with PEI were made by adding PEI to a solution of DNA followed by vortexing for about 1 min followed by incubation at room temperature for 30 min. The charge ratio R is the ratio of primary nitrogen of PEI to the phosphate of DNA. The ratio $R = 5.0$ was maintained for PEI experiments.

Steady state fluorescence spectra were recorded using a SPEX Fluorolog EL 111 T-format spectrofluorimeter. Time-resolved fluorescence measurements were carried out by time- correlated single-photon counting (TCSPC) method. A CW Nd:Vanadate (Millennia, Spectra Physics, USA) pumped mode-locked Ti-Sapphire laser with doubled tunable output was used for exciting the samples at 457 nm. The fluorescence emission at magic angle (54.7°) was dispersed in a monochomator and counted by a MCP PMT (R2809) and processed through a TCSPC setup. The instrument response function had a FWHM of ~40 ps.

Fluorescence intensity decays obtained at magic angle were deconvoluted with the instrument response function and analyzed as a sum of exponentials to get the mean fluorescence lifetime.

$$I(t) = \Sigma\alpha_i \exp(-t/\tau i)$$

where $I(t)$ is the fluorescence intensity collected at magic angle at time t and α_i is the amplitude of the ith lifetime τ_i such that $\Sigma\alpha_i = 1$.

Time-resolved fluorescence anisotropy decays were analyzed by the following equations

$$I_{\parallel}(t) = I(t)[1 + 2r(t)]/3 \quad (1)$$

$$I_{\perp}(t) = I(t)[1 - r(t)]/3 \quad (2)$$

$$r(t) = [I_{\parallel}(t) - I_{\perp}(t)]/[I_{\parallel}(t) + 2I(t)] = r_0 \Sigma\beta_i \exp(-t/\varphi_i) \quad (3)$$

where r_0 is the initial anisotropy and β_i is the amplitude of the ith rotational correlation time φ_i such that $\sum \beta_i = 1$.

$I_{||}$ and $I_{\perp}$ are the emission intensities collected at polarizations parallel and perpendicular, respectively to the polarization axis of the excitation beam. While analyzing the kinetics of anisotropy decay using Eqs. (1) and (2), values of α_i and τ_i (obtained from the analysis of $I(t)$) were kept fixed in order to reduce the number of floating parameters. This procedure results in better estimation of anisotropy decay parameters.

Dynamic light scattering experiments were performed on a DynaPro-MS800 dynamic light scattering instrument (Protein Solutions Inc., VA, USA) having an inbuilt Laser at 820 nm, by monitoring the scattered light at 90° with respect to irradiation direction. Buffer solutions were filtered carefully through 20 nm filters (Whatman Anodisc 13) to remove dust particles. The observed autocorrelation curves (at least 10 collections each collected for 10 s) were analyzed either by "Regularization" software or "DynaLS" software provided by the manufacturer of the instrument to generate a distribution of R_h.

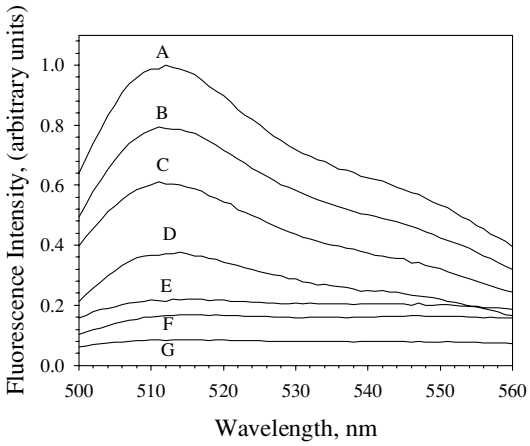

Fig. 1. Fluorescence emission spectra of DNA-YOYO-1 complex in the presence of 1 kD PEG, PEI, and 1 kD PEG + PEI. The concentrations of DNA (phosphate) and YOYO-1 were 3.7 μM and 75 nM, respectively (D:P = 1:50). The buffer used was 20 mM HEPES 500 mM NaCl pH 7.5. The excitation wavelength was 480 nm. A, no additive; B, 2.8 mg/mL PEG; C, 22.5 mg/mL PEG; D, 56.3 mg/mL PEG; E, 160 mg/mL PEG; F, 18.8 μM PEI; G, 160 mg/mL and 18.8 μM of PEG and PEI, respectively.

RESULTS AND DISCUSSIONS

Condensation of DNA Detected by YOYO-1

We had shown earlier that the bis-intercalating molecule YOYO-1 is a robust and convenient monitor of DNA condensation [11,15]. The fluorescence of DNA-bound YOYO-1 gets quenched when DNA condenses. It was also shown that quenching of fluorescence occurs only when sufficiently high level of YOYO-1 is bound to DNA (YOYO-1: nucleotide, D:P ~ 1:50) and the quenching was shown to be caused by the formation of excitonic H-type dimer of DNA-bound YOYO-1 [11]. Furthermore it was also shown that when low levels of YOYO-1 (D:P ~ 1:1000) were used, the fluorescence probe reported the dynamics of base and the backbone of DNA [11,15]. All these well-established monitors were used in this present work.

Figure 1 shows the effect of PEG on the fluorescence emission spectra of YOYO-1 bound to DNA at D:P ~1:50. The spectra show a steady decrease in fluorescence intensity with increasing concentration of PEG in the medium. Furthermore, the decrease in steady-state fluorescence intensity seen in the presence of PEG was also supported by a similar decrease observed in mean fluorescence lifetime (τ_m, Fig. 2). This is important in that τ_m is independent of concentration of the fluorophore and hence it is more robust in reporting the quenching of fluorescence. Since fluorescence quantum yield, φ is linearly related to τ_m ($\varphi = k_r\ \tau_m$, where k_r is the radiative rate constant) the observed similar behavior of fluorescence intensity and τ_m is quite satisfying. That the quenching of fluorescence (Figs. 1 and 2) is due to the condensation of DNA and not due to any other changes induced by the presence of PEG was shown by experiments in which the fluorescence was monitored at low levels of YOYO-1 (D:P ~ 1:10,000). In this situation both the intensity and τ_m did not show any significant

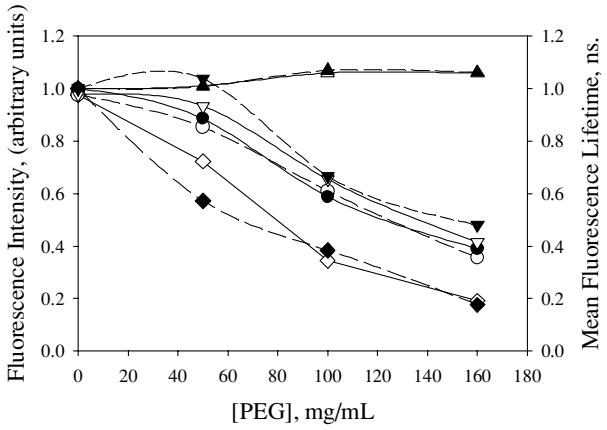

Fig. 2. Dependence of fluorescence intensity (closed symbols) and mean fluorescence lifetime (open symbols) of the DNA-YOYO-1 complexes on the concentration of PEG. D:P = 1:50 for all the samples except for the top curve (▲, △) for which D:P = 1:10,000 and 1 kD PEG. Inverted triangle, 10 kD PEG; Circles, 3.35 kD PEG; Diamonds, 1 kD PEG. Other experimental conditions are similar to those given in Fig. 1.

change in the presence of PEG (Fig. 2). Thus we see that the origin of quenching of fluorescence observed at high levels of YOYO-1 (Figs. 1 and 2) is the condensation of DNA.

The efficiency of condensation depends upon the polymer chain length of PEG as shown by the concentration dependence of normalized fluorescence intensity and mean lifetime (Fig. 2). PEG with an average mol. wt. of 1 kD showed higher efficiency when compared to PEG with average mol. wt. of 10 kD at comparable concentrations of PEG monomers (Fig. 2). These results may seem at variance with that observed by Vasilevskaya and coworkers [23] who showed that PEG with a degree of polymerization, $P = 454$ to be more effective when compared to a shorter ($P = 186$) polymer. However, we note the following differences between the two sets of experiments: (i) In our experiments, the value of P varies in the range of 20–200 in contrast to the studies by Vasilevskaya *et al*. and (ii) Vasilevskaya and coworkers [23] monitored the condensation of very long DNA at single molecule level from the change in the apparent molecular dimensions seen in fluorescence microscopic images. In contrast, we infer the condensation process from the quenching of fluorescence of DNA-bound YOYO-1 caused by interaction among YOYO-1 molecules bound to the same DNA molecule. Thus, the level of quenching will be governed by the *extent* of compaction in the condensed DNA. The extent of compaction, which is related to the extent of volume excluded by PEG, easily discernable from our measurements is unlikely to be detected within the resolution offered by the optical microscopic measurements of dimension of condensed DNA by Vasilevskaya and coworkers [23]. This and the fact that our measurements are ensemble-averaged observations could have caused the apparent difference mentioned above. In this connection, the observed opposing effects of PEG200 and PEG1540 on the unimolecular cyclization of DNA, which is assumed, to be similar to condensation of DNA is significant [34].

Condensation of DNA in the presence of PEG has been addressed theoretically by several workers [23,35–39]. One of the main indicators from these studies is the requirement of counterions for charge neutralization of DNA backbone during the process of condensation by osmotic exclusion agents. This is also seen in our experiments, which showed the requirement of salt for condensation (Fig. 3). Apart from the requirement of salt, we also see that the effect of various salts is not identical (Fig. 3). The variation in the efficiency of different salts in bringing about PEG-induced condensation indicates that the effect of salt lies in more than neutralization of phosphate charges of DNA backbone. It is likely that this difference

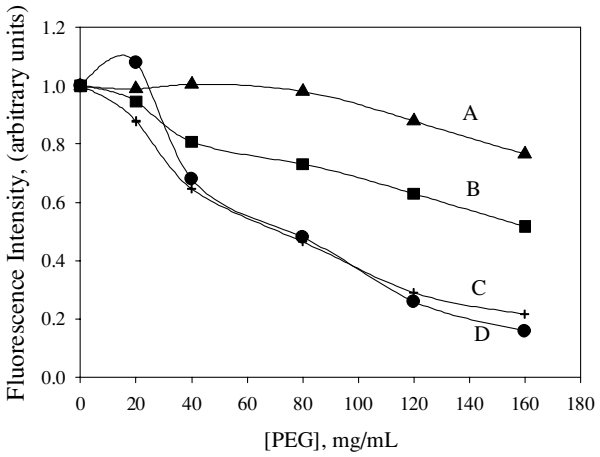

Fig. 3. Titration of fluorescence intensity of DNA- bound YOYO-1 with PEG in the presence of various salts. (A) In the absence of salt; (B) With 500 mM Na_2SO_4; (C) With 500 mM NaCl; (D) With 500 mM $NaNO_3$. The concentration of DNA (phosphate) and YOYO-1 were 3.7 μM and 75 nM, respectively (D:P = 1:50) in 20 mM HEPES pH 7.5. Other experimental conditions are similar to those given in Fig. 1.

is a reflection of other factors such as structure-forming and structure-breaking ability and osmotic effect offered by salt.

How does the structure of DNA condensed in the presence of PEG compare with the DNA condensed by binding agents such as polyethyleneimine (PEI) or a cationic detergent cetyltrimethylammonium bromide (CTAB). An indication toward the answer to this question can be provided from the extent of fluorescence quenching of YOYO-1 during condensation of DNA (Figs. 1 and 2). It is seen that the extent of quenching in the presence of PEI is significantly higher when compared to that of PEG samples. However, the extent of quenching by either the cationic detergent CTAB or PEG are very similar to each other (see Ref. [11]). Although the quantitative relationship between the extent of quenching and the extent of compaction is not known, the present results indicate that DNA condensed in the presence of PEG is less compact when compared to DNA condensed by PEI. This may be rationalized by noting that binding agents such as PEI could compact DNA very tightly due to its multidentate nature of binding. In contrast, agents such as PEG which works by volume exclusion by molecular crowding or CTAB, which works by neutralization of charge of DNA backbone, would rely on the inherent propensity of DNA polymer to self-aggregate. Thus our results suggest that DNA condensed by self-aggregation is less compact when compared to DNA condensed by cationic polymers. In order to obtain more comparative insight into the various

DNA condensates, we measured the rotational dynamics of DNA-bound YOYO-1 (see below).

Dynamics of Condensed DNA

Information on the dynamics of DNA base and backbone can be extracted from picosecond time-resolved fluorescence anisotropy of DNA intercalators such as ethidium [40] and YOYO-1 [11,15]. Fluorescence anisotropy decay of YOYO-1 is quite sensitive to changes in DNA backbone dynamics during condensation induced by either binding agents [11] such as PEI, CTAB, and Co^{3+} or the retroviral nucleocapsid protein NCp7 [15].

Figure 4 shows typical traces of decay kinetics of fluorescence anisotropy of DNA-bound YOYO-1. In these experiments, the ratio D:P was kept at 1:1000. As shown earlier (Fig. 2), under such low levels of the fluorescence probe, condensation of DNA does not cause the "signature" quenching of fluorescence intensity. This condition is essential to be kept when information on the changes in DNA dynamics is sought. The first inference from the data on fluorescence anisotropy decay kinetics (Fig. 4 and Table I) is the drastic change seen in the anisotropy decay profile in the presence of PEG. Analysis of decay curves by the nonassociative model [41,42] (see "Experimental Section") shows that, in the uncondensed DNA, the decay profile fits well to a sum of two exponentials, one <100 ps and another $\sim$7 ns (Table I). These values which are similar to those obtained in our earlier works [11,15] correspond to local motion of the fluorophore and segmental dynamics of DNA backbone, respectively. In these analyses the initial (or maximum) anisotropy was fixed at 0.31, the value obtained in experiments on YOYO-1 in viscous glycerol–water mixtures [11]. The significant change in the anisotropy decay kinetics in PEG-condensed DNA is seen in the longer correlation time which changed from $\sim$7 ns in the uncondensed form to 15–23 ns in DNA condensed by PEG (Table I). Since this correlation time has been identified with the segmental motion of DNA backbone [11,15], the condensation-induced increase in its value would indicate rigidfication of the backbone. That the long correlation time should be associated with segmental motion of the backbone rather than the overall tumbling dynamics of condensed DNA gets support when we note that the global tumbling dynamics of condensed DNA having $\sim$3000 basepairs is expected to be in the microsecond timescale.

Inspection of the value of the long correlation time (φ_3 in Table I) shows that the extent of rigidity of DNA backbone is higher in the presence of 1 kD PEG when compared to PEG of higher mol. wt. (3.35 kD or 10 kD). This observation is in line with the higher level of fluorescence quenching observed in the presence of 1 kD PEG when compared to longer polymers (Fig. 2). This may be due to the possibility that smaller polymers of PEG allow better invasion into the DNA. This could lead to an increase in the osmotic exclusion of water from the vicinity of DNA backbone. Furthermore, the longer value ($>$50 ns) of the correlation time observed in the presence of PEI correlates with the high level ($\sim$90%) of quenching shown by PEI. Thus we get a picture that the level of rigidfication of DNA backbone and the extent of DNA compaction are correlated with each other.

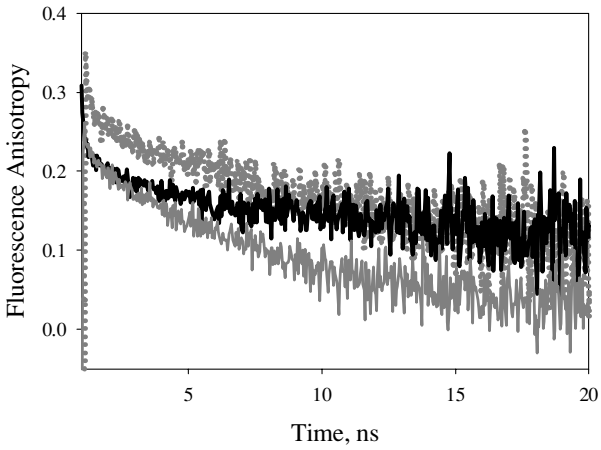

Fig. 4. Typical traces of decay of fluorescence anisotropy of DNA-YOYO-1 complexes. Grey continuous trace, uncondensed DNA; Dark continuous trace, DNA condensed by 1 kD PEG (160 mg/mL); Dotted trace, DNA in the presence of 28% glycerol having a bulk viscosity of 2.3 cP which is the same as that of 160 mg/mL 1 kD PEG. Rotational correlation times estimated from analysis of such traces are given in Table I.

PEG increases the bulk viscosity of solutions. For example, the bulk viscosity of a solution of 160 mg mL^{-1} of 1 kD PEG was 2.3 cP. Hence one could argue that the increase in the value of the long correlation time observed in the presence of PEG (Table I) could have arisen from the direct effect of increased solvent viscosity slowing down the segmental dynamics of the DNA backbone rather than a condensation-induced effect. Such an effect by bulk solvent is restricted by the relative molecular sizes of the probe and the viscogen. For example, when the bulk viscosity is increased by the addition of long chain polymers, the microviscosity felt by small molecular probes do not show any significant level of increase [41,43]. In contrast, when the sizes of viscogen and the probe are similar to each other, the microviscosity felt by the probe molecule nearly equals the bulk viscosity [41,43]. Such

Table I. Parameters Obtained from Analysis of Kinetics of Decay of Fluorescence Anisotropy of DNA-YOYO-1 Complexes

Sample[a]	Rotational correlation times, ns (amplitude)[b]		
	φ_1 (β_1)	ϕ_2 (β_2)	ϕ_3 (β_3)
DNA-YOYO-1	<0.1 (0.31)	—	7.3 (0.69)
DNA-YOYO-1 + PEI	<0.1 (0.35)	0.90 (0.15)	>50.0 (0.50)
DNA-YOYO-1 + 1 kD PEG	<0.1 (0.27)	1.00 (0.22)	23.1 (0.51)
DNA-YOYO-1 + 3.35 kD PEG	<0.1 (0.34)	3.6 (0.06)	14.6 (0.60)
DNA-YOYO-1 + 10 kD PEG	<0.1 (0.32)	3.1 (0.12)	14.8 (0.56)
DNA-YOYO-1 + 28% glycerol[c]	0.32 (0.26)	—	18.3 (0.74)

[a] The concentration of DNA (phosphate) and YOYO-1 were 30 μM and 30 nM, respectively (D:P = 1:1000). The buffer used was 20 mM HEPES 500 mM NaCl pH 7.46. PEG used was 160 mg/mL. The charge ratio for PEI (nitrogen): DNA (phosphate), $R = 5$.

[b] The errors associated with various parameters were as follows: φ_2 ($\pm$0.30), φ_3 ($\pm$2.0), β_1 ($\pm$0.03), β_2 ($\pm$0.03), and β_3 ($\pm$0.03). The value of reduced χ^2 was in the range of 1.0–1.4 in all the cases and the residual pattern was found to be random for all the fits. The initial anisotropy r_0 was fixed at 0.31 $\pm$ 0.01, the value obtained for YOYO-1 in glycerol, during the analysis.

[c] Viscosity of 28% glycerol is 2.3 cP which is the same as that of a solution of 160 mg mL^{-1} of 1 kD PEG.

observations have been ascribed to caging effect offered by bulky viscogens. In any case, in order to check whether the observed decrease in the long correlation time is due to the increase in solvent viscosity, we performed the experiment in the presence of glycerol, which increases the solvent viscosity. Moreover, 28% (v/v) glycerol has a bulk viscosity of 2.3 cP same as that of a solution of 160 mg mL^{-1} of 1 kD PEG. However, the fluorescence anisotropy decay kinetics of DNA-bound YOYO-1 was distinctly different in these two environments (Fig. 4 and Table I). Analysis of the decay curves show that the value of the longer rotational correlation time was ~18 ns (74%) in the presence of 28% glycerol. In contrast, the values were 1.0 ns (22%) and 23.1 ns (51%) in the presence of 1 kD PEG. Furthermore, the shortest correlation time (φ_1), which was ascribed to the internal motion of DNA-bound YOYO-1, was found to slow down significantly from <0.1 ns to 0.3 ns in the presence of 28% glycerol. This could be due to the effect of increase in the viscosity caused by the presence of glycerol. The absence of this effect (slowing down of the internal motion) in the presence of PEG (and in the other agents PEI, CTAB, and NCp7, see Refs. [11] and [15]) could be explained by the model, mentioned above, wherein the microviscosity is largely unaffected by long chain polymers. Furthermore, this observation shows that condensation of DNA, in general, does not perturb the internal motion of base-pairs. It was ensured that the presence of glycerol by itself does not lead to condensation of DNA as shown by the insignificant change in the fluorescence intensity of DNA-bound YOYO-1 (data not shown). Thus it clear that the rigidification of DNA backbone in the presence of PEG as inferred from the increase in the value of long correlation time is due to condensation of DNA.

Comparison of DNA Condensed by Binding Agents and Crowding Agents

Although condensation of DNA has a contribution from attractive interaction between DNA molecules, the overall mechanism of condensation aided by either binding agents such as PEI and CTAB or molecular crowding agents such as PEG is quite different from each other. This could lead to significant differences in the structure and dynamics of DNA condensed by these two classes of condensing agents. Quenching of fluorescence of bis-intercalated YOYO-1 which is a robust and convenient marker of DNA condensation [11,15] has shown clearly that DNA condensed by PEG is less compact when compared to DNA condensed by PEI (Figs. 1 and 2). In a parallel fashion, the backbone of DNA gets rigidified to a lesser extent on condensation by PEG when compared to the higher level of rigidification in PEI-induced condensates (Table I). The reduced level of compactness of DNA condensed by PEG when compared to DNA condensed by PEI was also demonstrated by the observation that the fluorescence intensity of PEG-DNA condensate got further reduced significantly by the addition of PEI (Fig. 1).

The difference in the size and the compactness of DNA condensates were evaluated by dynamic light scattering (DLS) experiments. For uncondensed DNA, the hydrodynamic radius, R_h estimated from DLS measurements was ~70 nm. DNA condensed by 1kD PEG

showed $R_h \sim 300$ nm which is significantly larger than the size of toroidal structures (50–100 nm) seen in AFM images of DNA condensed by PEI [33].

In conclusion, the observations presented in this work are very relevant in building models for understanding the compaction of DNA in chromosomes, phage heads, etc. In these situations, DNA has to be compacted for achieving economy of space while keeping intact the efficiency of DNA read-out in replication and transcription. The reduced level of compaction observed in the presence of PEG could be thought of as a strategy in achieving such apparently contradictory requirements.

ACKNOWLEDGMENTS

We thank Prof. N. Periasamy for providing us the software for analysis of time-resolved fluorescence data and Prof. B. J. Rao for his help in the extraction of plasmid DNA.

REFERENCES

1. G. Arents and E. N. Moudrianakis (1993). *Proc. Natl. Acad. Sci. USA*. **90**, 10489–10493.
2. J. A. Shellman and N. Parthasarathy (1984). *J. Mol. Biol.* **175**, 313–329.
3. D. Goula, C. Benoist, S. Mantero, S. Merlo, G. Levi, and B. A. Demeneix (1998). *Gene Ther.* **5**, 1291–1295.
4. A. Aris and A. Villaverde (2004). *Trends Biotechnol*. **22**, 371–377.
5. H. Petry, C. Goldmann, O. Ast, and W. Luke (2003). *Curr. Opin. Mol. Ther.* **5**, 524–528.
6. A. El Aneed (2004). *J. Control Release* **94**, 1–14.
7. K. Minagawa, Y. Matsuzawa, K. Yoshikawa, A. R. Khokhlov, and M. Doi (1994). *Biopolymers* **34**, 555–558.
8. V. A. Bloomfield (1996). *Curr. Opin. Struct. Biol.* **6**, 334–341.
9. J. P. Behr (1993). *Acc. Chem. Res.* **26**, 274–278.
10. M. X. Tang and F. C. Szoka (1997). *Gene Ther.* **4**, 823–832.
11. G. Krishnamoorthy, G. Duportail, and Y. Mely (2002). *Biochemistry* **41**, 15277–15287.
12. A. D. Miller (1998). *Angew. Chem. Int. Ed.* **37**, 1768–1785.
13. Y. S. Tarahovsky, V. A. Rakhmanova, R. M. Epand, and R. C. MacDonald (2002). *Biophys. J.* **82**, 264–273.
14. S. M. Mel'nikov, V. G. Sergeyev, Y. S. Melnikova, and K. Yoshikawa (1997). *J. Chem. Soc. (Faraday Trans.)* **93**, 283–288.
15. G. Krishnamoorthy, B. Roques, J-L. Darlix, and Y. Mely (2003). *Nucleic Acids Res.* **31**, 5425–5432.
16. P. G. Arscott, C. Ma, J. R. Wenner, and V. A. Bloomfield (1995). *Biopolymers* **36**, 345–364.
17. R. Marquet and C. Houssier (1991). *J. Biomol. Struct. Dyn.* **9**, 159–167.
18. V. A. Bloomfield (1997). *Bioplymers* **44**, 269–282.
19. D. C. Rau and V. A. Parsegian (1992). *Biophys. J.* **61**, 246–271.
20. Y. Fang and J. H. Ho (1998). *Nucleic Acids Res.* **26**, 588–593.
21. L. Lerman (1971). *Proc. Natl. Acad. Sci. USA*. **68**, 1886–1890.
22. S. R. Seth and D. Leckband (1997). *Proc. Natl. Acad. Sci.* **94**, 8399–8404.
23. V. V. Vasilevskaya, A. R. Khokhlov, Y. Matsuzawa, and K. Yoshikawa (1995). *J. Chem. Phys.* **102**, 6595–6602.
24. K. Yoshikawa (2001). *Adv. Drug Deliv. Rev.* **52**, 235–244.
25. A. N. Naimushin, N. Quach, B. S. Fujimoto, and J. M. Schurr (2001). *Biopolymers* **58**, 204–217.
26. N. Tokuriki, M. Kinjo, S. Negi, M. Hoshino, Y. Goto, I. Urabe, and T. Yomo (2004). *Protein Sci.* **13**, 125–133.
27. A. Minton (2000). *Curr. Opin. Struct. Biol.* **10**, 34–39.
28. A. Minton (2001). *J. Biol. Chem.* **276**, 10577–10580.
29. R. J. Ellis (2001). *Trends Biochem. Sci.* **26**, 597–604.
30. D. Fischer, T. Bieber, Y. Li, H.-P. Elsasser, and T. Kissel (1999). *Pharm. Res.* **16**, 1273–1279.
31. M. H. Kombrabail and G. Krishnamoorthy (2003). *J. Fluoresc.* **13**, 339–347.
32. D. Porschke (1984). *Biochemistry* **41**, 15277–15287.
33. D. D. Dunlap, A. Maggi, M. R. Soria, and L. Monaco (1997). *Nucleic Acids Res.* **25**, 3095–3101.
34. L. Donna and P. Serwer (1994). *J. Mol. Biol.* **242**, 547–558.
35. J. Naghizadeh and A. R. Massih (1978). *Phys. Rev. Lett.* **40**, 1299–1302.
36. C. B. Post and B. H. Zimm (1979). *Biopolymers* **18**, 1487–1501.
37. H. L. Frisch and S. J. Fesciyan (1979). *J. Polym. Sci. Polym. Lett. Ed.* **17**, 309–315.
38. A. Y. Grosberg, I. Y. Erukhimovich, and E. I. Shakhnovich (1981). *Biophyics (USSR)* **26**, 415–420.
39. A. Y. Grosberg, I. Y. Erukhimovich, and E. I. Shakhnovich (1981). *Biophysics (USSR)* **26**, 897–905.
40. J. M. Schurr, B. S. Fujimoto, P. Wu, and L. Song (1992). In J. R. Lakowicz (Ed.), *Topics in Fluorescence Spectroscopy*, Vol. 3, Plenum, New York, pp. 137–229.
41. A. Srivastava and G. Krishnamoorthy (1997). *Arch. Biochem. Biophys.* **340**, 159–167.
42. J. R. Lakowicz (2000). *Principle of Fluorescence spectroscopy*, Plenum, New York.
43. K. Luby-Phelps, S. Mazumdar, R. B. Mazumdar, L. A. Earnst, W. Galbraith, and A. S. Waggoner (1993). *Biophys. J.* **65**, 236–242.